Photon management with index-near-zero materials

Zhu Wang, Ziyu Wang, and Zongfu Yu

Citation: Applied Physics Letters **109**, 051101 (2016); doi: 10.1063/1.4960150
View online: http://dx.doi.org/10.1063/1.4960150
View Table of Contents: http://scitation.aip.org/content/aip/journal/apl/109/5?ver=pdfcov
Published by the AIP Publishing

Photon management with index-near-zero materials

Zhu Wang,[1] Ziyu Wang,[2] and Zongfu Yu[1]
[1]*Department of Electrical and Computer Engineering, University of Wisconsin Madison, Madison, Wisconsin 53706, USA*
[2]*Department of Foundation, Southeast University, Chengxian College, 210018 Nanjing, China*

(Received 29 February 2016; accepted 19 July 2016; published online 1 August 2016)

Index-near-zero materials can be used for effective photon management. They help to restrict the angle of acceptance, resulting in greatly enhanced light trapping limit. In addition, these materials also decrease the radiative recombination, leading to enhanced open circuit voltage and energy efficiency in direct bandgap solar cells. *Published by AIP Publishing.* [http://dx.doi.org/10.1063/1.4960150]

The goal of photon management is to increase the efficiency of solar energy conversion through enhanced light-matter interactions. High-index materials have been long advocated for this purpose[1] because their high optical density of states (DOS) creates strong light-matter interactions[2–4] through absorption and scattering. Specifically, the technique of light trapping has been developed to exploit high-index materials to increase the optical path length in solar absorbers. Figure 1(a) shows the classical setup of light trapping. An absorber with a refractive index n is placed on the top of a Lambertian mirror. When incident sunlight passes through the absorber and reaches the mirror, the reflection direction is randomized. Light rays with large reflection angles propagate for longer distances. They can even go through multiple reflections to accumulate optical paths that are much longer than the absorber thickness d. A longer path indicates stronger light absorption, which is desirable for solar cells. Yablonovitch developed a statistical ray optics theory and showed that the average path length l_e is subject to the light-trapping limit[2] F

$$F = \frac{l_e}{d} \leq 4n^2.$$

It shows that a higher index material could create longer light-trapping paths and therefore stronger light absorption. High-index materials, such as Si and GaAs, afford a much better light-trapping performance than the low-index ones, such as polymers. The understanding of this light-trapping limit has significantly contributed to the development of high-efficiency solar cells in the past decades. It has been generally believed that low-index materials are undesirable for photon management.

Here, we show that an emerging optical material with ultra-low DOS could provide a different way of realizing strong light-matter interactions. These materials, also named index-near-zero (INZ) materials,[5–12] have refractive indices smaller than vacuum. Intriguing effects have been found in INZ materials such as cloaking,[13,14] bending with small curvature,[15–17] and super scattering.[18] Here, we show that INZ materials also exhibit exciting potentials to realize light-trapping performance far better than the conventional limit. Moreover, INZ materials can also improve the photovoltaic voltage owing to the reduced radiative emission. Such voltage enhancement cannot be realized by conventional high-index materials. It can achieve significant enhanced efficiency for direct bandgap solar cells under one sun.[19]

We start by using a ray-tracing theory to show the fundamental limit of light trapping in INZ materials. Figure 1(b) shows a solar absorber with a cladding layer of the INZ material. The absorber is made from conventional semiconductors. It is placed on a perfect Lambertian mirror. Perfect anti-reflection is used at all interfaces. We will show that the INZ material increases the light-trapping limit to

$$F \leq \frac{4n^2}{{n_{inz}}^2}, \tag{1}$$

where n_{inz} is the index of the INZ material. With an index $n_{inz} \ll 1$, this limit can go far beyond the Yablonovitch limit $4n^2$. For instance when $n_{inz} = 0.1$, the limit is $400n^2$. It is two orders of magnitude higher than the conventional Yablonovitch limit $4n^2$, indicating extraordinarily long optical paths and strong sunlight absorption in the absorber.

To prove the above limit, we trace the path of a normally incident light ray. It first travels a distance of d to reach the bottom mirror as shown in Fig. 1(b). Then, it is reflected by the diffusive mirror and propagates in a random direction θ. The path length of the reflected light is $d/\cos\theta$ when it reaches the INZ-absorber interface. Considering the randomness of the reflection angle, we can calculate the average light path as

$$\frac{\int\int \frac{d}{\cos\theta}\cos\theta d\Omega}{\int\int \cos\theta d\Omega} = 2\mathrm{d}.$$

Here, the probability distribution of the reflection angle is $\cos\theta/(\int\int \cos\theta \mathrm{d}\Omega)$ and the $\cos\theta$ factor accounts for the power distribution reflected by a Lambertian surface. Not all light that reaches the INZ-absorber interface can escape to the outside. Total internal reflection defines an escape cone with an apex angle of $\theta_c = \sin^{-1}(n_{inz}/n)$ as shown by the brown cone in Fig. 1(b). The reflected light can escape only when $\theta < \theta_c$. The probability of such an event is n_{inz}^2/n^2 (details in supplementary material[20]). For $\theta \geq \theta_c$, light is trapped and propagates toward the Lambertian mirror which randomizes its direction again. By tracing the path in an infinite series of reflections, we obtain the average light path length

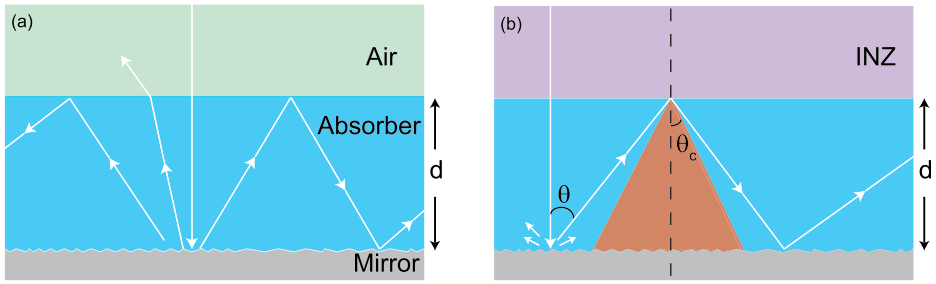

FIG. 1. (a) Schematic of conventional light-trapping. The solar absorber (blue color in the middle) is placed on top of a perfect Lambertian mirror (gray at the bottom). (b) Schematic of ray-tracing theory. The INZ material is represented by the purple color on the top. Light rays are represented by white arrows.

$$l_e = d + 2d + 4d\left(1 - \frac{{n_{inz}}^2}{n^2}\right) + 4d\left(1 - \frac{{n_{inz}}^2}{n^2}\right)^2 + \cdots = \left(\frac{4n^2}{{n_{inz}}^2} - 1\right)d.$$

Here, we have neglected the absorption loss, following the standard assumption used in deriving the light-trapping limit. The above equation directly leads to the limit in Eq. (1). This ray-tracing theory shows that conventional high-index absorbers improve conventional light trapping because a high-index n reduces the size of the escape cone $\sin^{-1}(n_{inz}/n)$. Here, INZ materials introduce an alternative way to reduce the escape cone by using $n_{inz} < 1$.

The ray-tracing theory is intuitive. However, many INZ materials and thin-film absorbers heavily rely on nanostructures. The optical interferences and diffraction make it difficult to treat light as rays. In addition, the light-trapping limit in nanostructures also differs from the conventional Yablonovitch limit.[3] Next, we use rigorous wave theory to show the limit of light trapping when INZ materials are used with nanostructured materials.

Without loss of generality, we consider a periodic nanostructured absorber with a period of L. Non-periodic structures can be understood by taking the limit of $L \to \infty$. The wave effects make it impossible to trace the light path. To overcome this issue, we first calculate the absorption enhancement factor $\mathbb{F} = A/\alpha d$, where A and d are the absorptance and the average thickness of the absorber, respectively. α is the intrinsic absorption coefficient of the material. The light-trapping limit, i.e., the maximum enhancement of light path length F, can then be obtained by[3]

$$F = \lim_{\alpha d \to 0} \mathbb{F}.$$

In the weak absorption limit when $\alpha d \to 0$, light absorption A is linearly proportional to the light path length l. Therefore, the absorption enhancement factor $\mathbb{F}$ provides a direct measure of the light-trapping limit F.

There is another wonderful consequence as $\alpha d \to 0$: all light absorption is contributed by optical resonance. Non-resonant absorption can be safely neglected. As a result, light absorption can be conveniently evaluated by the summation of the absorption of all resonances. For a single resonance, the maximum broadband absorption is $\sigma_{max} = \int_0^\infty A(\omega)d\omega = 2\pi\gamma/N$, where N is the number of diffraction beams created by the periodic nanostructure. γ is the intrinsic absorption rate of the resonance, defined by the ratio between the amount of light energy absorbed per unit of time and the total energy stored in the resonance. As a good approximation, $\gamma = \alpha c/n$ with c being the speed of light in vacuum. The light absorption is simply the summation of the absorption by all resonances $A = M\sigma_{max}/\Delta\omega$, where M is the total number of resonances in the spectral range between ω and $\omega + \Delta\omega$. The upper limit of light absorption enhancement can be calculated as[3]

$$\mathbb{F} = \frac{A}{\alpha d} = \frac{2\pi\gamma}{\alpha d \Delta\omega} \times \frac{M}{N}. \quad (2)$$

Eq. (2) applies to both bulk and nanostructured absorbers. For bulk absorbers, one can use the standard bulk DOS to calculate the number of resonances $M_{bulk} = \frac{8\pi n^2 \omega^3}{c^3}\left(\frac{L}{2\pi}\right)^2\left(\frac{d}{2\pi}\right)\Delta\omega$, which would reproduce the conventional $4n^2$ limit. In the nanostructures, previous research efforts have mainly focused on designing the DOS of nanostructured absorbers such that it exceeds M_{bulk}.[3,4] Here, INZ materials realize enhancement through a completely different mechanism. They do not enhance the DOS and M. Instead, their ultra-low index significantly reduces the number of diffraction beams N.

We first briefly review the impact of N on light trapping based on the case without INZ materials.[21] The diffraction beams created by a periodic nanostructure can be described by a set of plane waves shown by the dots in the k-space in Fig. 2(a). They are spaced by $\Delta k = 2\pi/L$. N is the number of dots inside the propagating-wave circle of a radius k_0 (red area in Fig. 2(a)). Outside the circle are the evanescent waves. The light-trapping limit strongly depends on the period L because L dictates the density of dots in the k-space. Such wave effect is absent in the ray-tracing theory. As the period L increases, N increases in steps (red lines in Fig. 2(b)) while the number of resonance per unit cell M also increases. The resulting light trapping limit can be calculated from Eq. (2) and is shown by the red lines in Fig. 2(c). When the period is around wavelength $L/\lambda \sim 1$, the light-trapping limit deviates significantly from the bulk $4n^2$ limit. When $L/\lambda \gg 1$, the limit approaches the ray-tracing limit $4n^2$, which is expected because the wave effects are less pronounced in large-period structures.

Next, we evaluate how INZ materials affect the above wave-based analysis. With an INZ material above the nanostructured absorber, the radius of the propagating-wave circle is reduced by a factor of n_{inz} (blue area in Fig. 2(a)). Consequently, there are fewer diffraction beams (blue lines in Fig. 2(b)) while the number of resonances M remains the same because the absorber is the same. As a result, the light-trapping limit is higher than that without the INZ material (blue lines in Fig. 2(c)). Again, as the period increases, the limit converges to $4n^2/n_{inz}^2$, which agrees excellently with the ray-tracing theory. We also derive the light-trapping limit

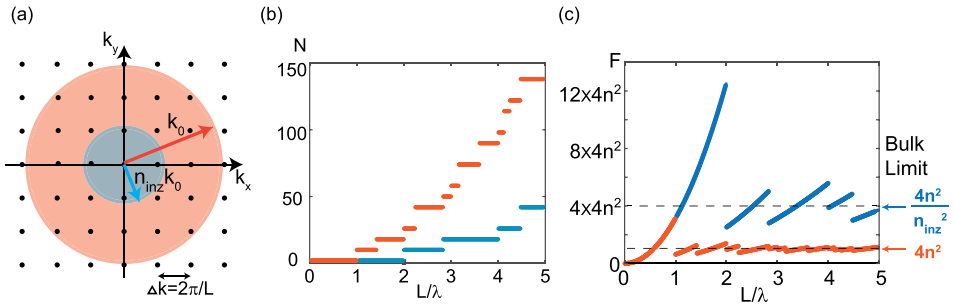

FIG. 2. (a) Schematic of the k-space for deriving the nanophotonic light-trapping limit. Dots represent all waves that satisfy the boundary condition. The index of the material above the absorber defines a circle where propagating wave can escape. The circle for vacuum (red) is larger than that for an INZ material (blue). (b) The number of diffraction beams N for the cases with vacuum (red) and an INZ material (blue) above the absorber. $n_{inz} = 0.5$. (c) Nanophotonic light-trapping limit with vacuum (red) and an INZ material (blue).

for INZ materials in 2-dimensional space, which is shown in the supplementary material.[20]

To validate the theory described above, we simulate light absorption by numerically solving the full-wave Maxwell's equations. While the enhancement is intrinsically broadband, we consider a normalized spectral range between λ_0 to $1.15\lambda_0$ to reduce the required computational resources. The structure of the simulated solar cell is shown in Fig. 3(a). It consists of an absorber with a thickness of $d = 5\lambda_0$ with the surface structure of the unit cell shown in Fig. 3(b) (details in supplementary material[20]). The period is $L = 3\lambda_0$. It is weakly absorptive with $\alpha d = 0.0006$. Such weakly absorptive material is often used to numerically test the limit of light trapping.[3] The absorber is placed on top of a mirror and below an INZ thin film with 1.7 λ_0 thickness. The refractive indices for the absorber and the INZ material are $n = 3.5$ and $n_{inz} = 0.33$, respectively. Anti-reflection layers are used at interfaces. We use the $S4$ method[22] to calculate the light absorption for normally incident light. The script of input files and detailed results are available online.[23] Comparing to the single path absorption αd, the polarization-averaged enhancement factor $\mathbb{F}$ is shown in Fig. 3(c). The spectrum consists of many sharp peaks caused by numerous resonances in the structure. The average absorption enhancement is $\overline{\mathbb{F}} = 823$, which agrees with the theoretical upper limit 1226 reasonably well. In comparison, the enhancement factor of the Yablonovitch limit is only 49. The INZ material increases the light-trapping limit by more than one order of magnitude, and it is higher than any light-trapping limit reported so far.

The light-trapping limit discussed above only concerns about the light absorption, which mainly helps to improve the photocurrent of solar cells. Here below we show that INZ materials can also improve another important property of solar cells: the open-circuit voltage. Specifically, the small phase space in INZ materials reduces the radiative emission. This decreased emission can be intuitively understood by considering a perfect blackbody placed inside an INZ material. The density of thermal radiation energy is $n_{inz}^2 \sigma T^4$ with σ and T being the Stefan-Boltzmann constant and the temperature, respectively. This emitted power is n_{inz}^2 times lower than the standard Stefan-Boltzmann law in vacuum. The same emission reduction also occurs in semiconductors, where INZ materials decrease the radiative recombination rate of photo-generated carriers.

For a specific example, we study GaAs cells as shown in the inset in Fig. 4(a). For simplicity, all dimensions of the solar cells are taken to be much larger than both the optical wavelengths as well as the absorption length of GaAs. We also exclude all non-idealities such as non-radiative recombination and interfacial reflections. These assumptions are standard in deriving the fundamental limit of the energy efficiency in direct bandgap solar cells and they are well justified in realistic high-quality GaAs cells.[24] Following the detailed balance analysis, the carrier generation rate F_g created by the sun must equal the recombination rate[19]

$$F_g = I + \exp\left(\frac{eV_{oc}}{k_B T}\right) F_o, \tag{3}$$

where e and k_B are the elementary charge and the Boltzmann constant, respectively. I is the current. The generation rate F_g is

$$F_g = \int_{E_g/\hbar}^{\infty} S(\omega) d\omega, \tag{4}$$

where $S(\omega)$ is the photon flux density from the sun and E_g is the bandgap energy of the semiconductor. On the right hand side of Eq. (3), F_o is the flux density of photons emitted by

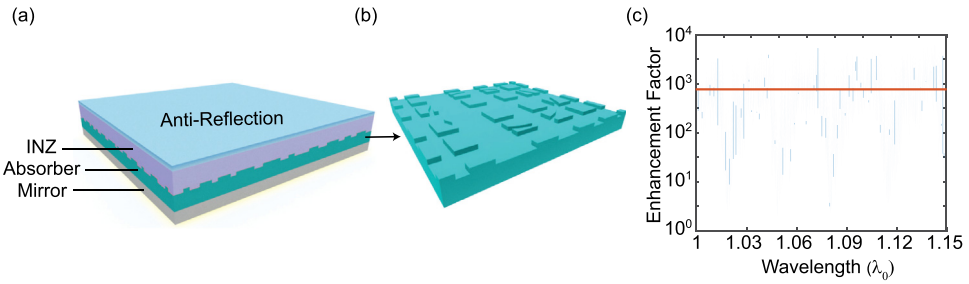

FIG. 3. (a) The periodic nanostructure used for simulation. (b) The surface structure of the absorber shown in (a). (c) The spectrum of the light absorption enhancement factor for the structure shown in (a).

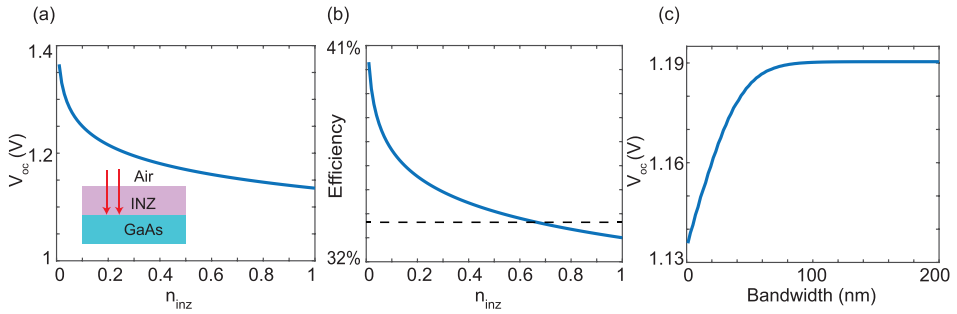

FIG. 4. (a) Calculated V_{oc} as a function of n_{inz} for ideal GaAs solar cells with a cladding of INZ material. GaAs absorber is thick enough to absorb all incident light and is placed on a mirror. (b) Maximum efficiency as a function of the index of the cladding INZ material. The Shockley-Queisser limit of energy conversion efficiency is indicated by the dashed line (c) V_{oc} as a function of the bandwidth of the INZ material. Inside the spectral bandwidth $n_{inz} = 0.33$ while outside $n_{inz} = 1$.

the absorber as a result of thermal fluctuation at the thermal equilibrium[25–27]

$$F_o = 2\pi \int_0^{\theta_c} d\theta \int_{E_g/\hbar}^{\infty} d\omega \cos\theta \sin\theta \Theta(T,\omega), \tag{5}$$

where $\Theta(T,\omega) = \frac{n^2\omega^2}{4c^2\pi^3}[\exp(\frac{\hbar\omega}{kT_c} - 1)]^{-1}$ is the thermal photon flux density in the absorber. It is important to note that the integration starts from the normal direction $\theta = 0$ to the critical angle $\theta_c = \sin^{-1}(n_{inz}/n)$. For photons' directions $\theta > \theta_c$, there will be complete photon recycling and it does not contribute to the radiative recombination.

Combining Eqs. (3)–(5), we can solve for the current-voltage relationship. Using GaAs at the open circuit condition $I = 0$, we calculate the open circuit voltage V_{oc} as a function of n_{inz} (Fig. 4(a)). When $n_{inz} = 1$, the result is identical to conventional detailed balance modeling, which produces the result from the standard Shockley-Queisser analysis. As n_{inz} decreases, the open circuit voltage increases. For example, when $n_{inz} = 0.1$, V_{oc} increases by more than 100 mV (Fig. 4(a)). As a result of the increased V_{oc}, the efficiency of energy conversion also increases. As shown in Fig. 4(b), it reaches over 40% for small indices. The use of INZ materials increases the energy conversion efficiency well above the Shockley-Queisser limit[19] of 33.7% for single-junction solar cells under one sun, which is indicated by the dashed line in Fig. 4(b).

Finally, we comment on the optical loss and spectral bandwidth of INZ materials. Lossless INZ materials were recently demonstrated[17,28] in structured dielectric materials. They do not use metals and thus are free from any light absorption. Even for those INZ materials that do use metals, rapid progress has been made toward low loss INZ materials.[29,30] While broadband INZ materials[31,32] are emerging, it is also important to emphasize that one does not need broadband INZ material to realize all the enhancement effects shown above. Because most radiative recombination occurs in the close vicinity of the bandgap frequency, a narrow band INZ would be equally effective in improving the open circuit voltage. As shown in Fig. 4(c), we use an index $n_{inz} = 0.33$ with a limited bandwidth in the frequency range right above $E_g/\hbar$. Even a 50 nm wavelength bandwidth produces an impressive enhancement of V_{oc}.

In conclusion, we show that INZ materials can be used for realizing strong light-matter interactions. Unlike conventional approaches that use high optical DOS, we exploit the ultra-low DOS in INZ materials to confine light in the absorbers. It is known that restricting the angular response of a solar cell improves the performance of photon management.[2,33–35] INZ materials provide a concrete implementation of this general principle. They accomplish effective angular concentration by using internal small phase spaces instead of bulk components such as lenses. As a result, they are much easier to integrate to accommodate diverse cell geometries. Similarly, INZ materials can also be used to improve the performance of other optoelectronic devices that require strong light-matter interactions, such as photodetectors and modulators.

This work was supported by NSF ECCS Award Number 1405201.

[1]M. L. Brongersma, Y. Cui, and S. Fan, Nat. Mater. **13**, 451 (2014).
[2]E. Yablonovitch, J. Opt. Soc. Am. **72**, 899 (1982).
[3]Z. Yu, A. Raman, and S. Fan, Proc. Natl. Acad. Sci. U.S.A. **107**, 17491 (2010).
[4]D. M. Callahan, J. N. Munday, and H. A. Atwater, Nano Lett. **12**, 214 (2012).
[5]A. Alù, M. G. Silveirinha, A. Salandrino, and N. Engheta, Phys. Rev. B **75**, 155410 (2007).
[6]S. Vassant, A. Archambault, F. Marquier, F. Pardo, U. Gennser, A. Cavanna, J. L. Pelouard, and J. J. Greffet, Phys. Rev. Lett. **109**, 237401 (2012).
[7]N. Engheta, Science **340**, 286 (2013).
[8]R. Maas, J. Parsons, N. Engheta, and A. Polman, Nat. Photonics **7**, 907 (2013).
[9]P. Moitra, Y. Yang, Z. Anderson, I. I. Kravchenko, D. P. Briggs, and J. Valentine, Nat. Photonics **7**, 791 (2013).
[10]S. Molesky, C. J. Dewalt, and Z. Jacob, Opt. Express **21**, A96 (2013).
[11]A. A. Basharin, C. Mavidis, M. Kafesaki, E. N. Economou, and C. M. Soukoulis, Phys. Rev. B **87**, 155130 (2013).
[12]J. Luo, W. Lu, Z. Hang, H. Chen, B. Hou, Y. Lai, and C. T. Chan, Phys. Rev. Lett. **112**, 73903 (2014).
[13]Y. Xu and H. Chen, Appl. Phys. Lett. **98**, 113501 (2011).
[14]L.-Y. Zheng, Y. Wu, X. Ni, Z.-G. Chen, M.-H. Lu, and Y.-F. Chen, Appl. Phys. Lett. **104**, 161904 (2014).
[15]M. Silveirinha and N. Engheta, Phys. Rev. Lett. **97**, 157403 (2006).
[16]B. Edwards, A. Alù, M. E. Young, M. Silveirinha, and N. Engheta, Phys. Rev. Lett. **100**, 33903 (2008).
[17]X. Huang, Y. Lai, Z. H. Hang, H. Zheng, and C. T. Chan, Nat. Mater. **10**, 582 (2011).
[18]M. Zhou, L. Shi, J. Zi, and Z. Yu, Phys. Rev. Lett. **115**, 23903 (2015).
[19]W. Shockley and H. J. Queisser, J. Appl. Phys. **32**, 510 (1961).
[20]See supplementary material at http://dx.doi.org/10.1063/1.4960150 for detailed analysis.
[21]Z. Yu, A. Raman, and S. Fan, Opt. Express **18**, A366 (2010).
[22]V. Liu and S. Fan, Comput. Phys. Commun. **183**, 2233 (2012).

[23]See https://en-real.com/tutorials/s4/IndexNearZeroSolarCells for simulation script.
[24]O. D. Miller, E. Yablonovitch, and S. R. Kurtz, IEEE J. Photovoltaics **2**, 303 (2012).
[25]A. Niv, M. Gharghi, C. Gladden, O. D. Miller, and X. Zhang, Phys. Rev. Lett. **109**, 138701 (2012).
[26]J. N. Munday, J. Appl. Phys. **112**, 64501 (2012).
[27]S. Sandhu, Z. Yu, and S. Fan, Opt. Express **21**, 1209 (2013).
[28]Y. Li, S. Kita, P. Muñoz, O. Reshef, D. I. Vulis, M. Yin, M. Lončar, and E. Mazur, Nat. Photonics **9**, 738 (2015).
[29]S. Campione, M. Albani, and F. Capolino, Opt. Mater. Express **1**, 1077 (2011).
[30]L. Sun, X. Yang, and J. Gao, Appl. Phys. Lett. **103**, 201109 (2013).
[31]L. Sun and K. W. Yu, J. Opt. Soc. Am. B **29**, 984 (2012).
[32]L. Sun, J. Gao, and X. Yang, Phys. Rev. B **87**, 165134 (2013).
[33]Z. Yu, A. Raman, and S. Fan, Appl. Phys. A **105**, 329 (2011).
[34]E. D. Kosten, J. H. Atwater, J. Parsons, A. Polman, and H. A. Atwater, Light Sci. Appl. **2**, e45 (2013).
[35]J. G. Mutitu, S. Shi, A. Barnett, and D. W. Prather, IEEE Photonics J. **2**, 490 (2010).